Supplementary Discussion

Quantitative analysis on the level of faithful carbon replication

The 'quality' of carbon replication of the zeolite can be evaluated by the quantitative analyses of gravimetric yield, volume conversion yield and pore size distribution. For instance, La^{3+}-exchanged FAU(X) zeolite yielded 0.31 ~ 0.32 g carbon/g zeolite, no matter whether the zeolite particle diameter was ~ 1 μm or 30 μm. The La-FAU(X) zeolite has a crystal density of 1.53 g/cm^3. Hence, the specific volume of the resultant zeolite-carbon composite crystal can be calculated as 1.00 cm^3/ (1.53 g zeolite + 0.31 g carbon) = 0.65 cm^3/g (zeolite + carbon). In the case of a perfect quality replicated carbon, the zeolite crystal volume and morphology should be fully retained by carbon frameworks even after the zeolite portion was completely dissolved. Therefore, assuming 100% volume yield, the volume of 0.65 cm^3 can be regarded as fully occupied by 0.31 g of carbon. Then, the pore volume possessed by the carbon becomes to 0.65 cm^3 – (0.31 g ÷ 1.56 g/ cm^3) = 0.45 cm^3. From this value, the pore volume per carbon mass can be calculated as 0.44 cm^3/ 0.31 g = 1.45 cm^3/g. In this calculation, the apparent density of carbon framework (including inaccessible internal pores, similar to the core of a closed carbon nanotube) was taken as 1.56 g/ cm^3 after the measurement using He pycnometry.

The calculated pore volume can be compared with the measured pore volume, which is actually determined from the t-plot analysis of the argon adsorption isotherm. In the present study, the isotherm analysis was performed using the non-linear density functional theory method. The pore volume, determined in this manner, is 1.2 cm^3/g^{-1} carbon. Dividing this result by the above calculated value of 1.4 cm^3 g^{-1} gives a ratio of 0.86. This ratio corresponds to a volume conversion yield of 83%. The actual conversion can be higher than 83% since the He pycnometric measurement can overestimate carbon density (helium atom is smaller than argon). For more detailed quantitative analysis on the "quality" of the carbon replication, the carbon pore size distribution in Figure S3 can be classified into three categories: diameters less than 1.3 nm as faithfully templated pores, 1.3~2.2 nm as partially templated pores, and greater than 2.2 nm as defective pores. Pore volumes corresponding to the three categories are 0.61, 0.28 and 0.31 cm^3 g^{-1}, respectively. Their ratios are 7.4: 1.8: 0.8. From these ratios, it can be estimated that 74% of the zeolite pores become 'completely faithful carbon replication'. The remainder of the zeolite pores correspond to 'partially faithful carbon replication' or 'empty pore region'. This estimation is consistent with the 83% volume yield obtained above.

In a simple diffusion-controlled chemical vapor deposition process, the deposition quantity increases sharply during the initial period, and afterwards, gradually reaches a saturation point. Unlike the simple diffusion-controlled CVD process, the carbon infiltration in the present zeolite follows an S-shape breakthrough curve exhibiting an initial induction period (shown in Extended Data Figure 2 of the main paper). The S-shape curve suggests that the carbon deposition can occur through nucleation, growth and termination processes, similar to the catalytic growths of single-walled carbon nanotube, or other crystal growths. The S-shape

curve indicates that the seed generation is slow. Once seeds are generated, however, local carbon growths around the seeds occur very rapidly. This process seems to fill zeolite pores very quickly, and this process may be referred to as a 'rapid spot growth' mechanism. The carbon growth is believed to proceed very rapidly by a radical mediated pyro-condensation polymerization route. This process seems to be catalyzed by La^{3+}, Y^{3+}, Ca^{2+} and so on. In this process, the carbon product collected in the first half of the breakthrough curve should have the same structural properties as the carbon obtained in the second half of the curve. The carbon formation stops when all diffusion pathways for ethylene (or acetylene) become completely blocked due to carbon in the neighboring pores. Based on the volume yield analysis, it may be concluded that the diffusion pathways could be completely closed when approximately 80% of the zeolite pores were filled with carbon. The carbon yield was the same, no matter whether the zeolite particle diameter was 1-μm small or 30-μm large. This result signifies the importance of the internal growth effects, rather than external diffusion or the size of crystals. In principle, without external diffusion limitations, the carbon synthesis can be readily scaled up to a very large batch size.
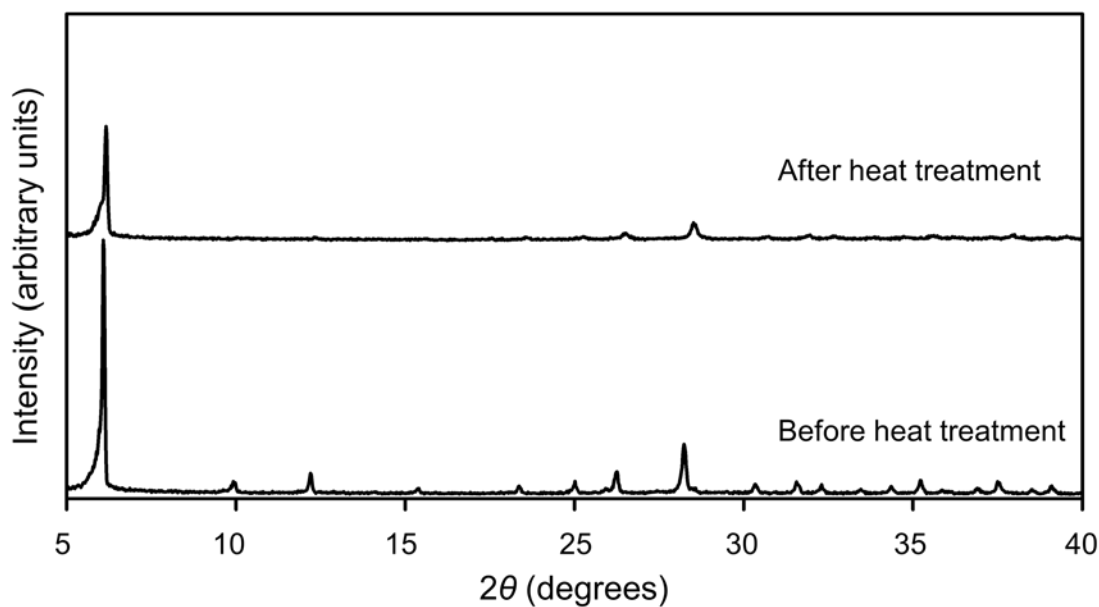
Supplementary Figures

Figure S1. XRD patterns for the 600 ºC carbon-deposited zeolite FAU, before and after heating to 850 ºC under N$_2$. The result indicates a significant contraction of the zeolite framework due to the heat treatment. In addition, some reflections are missing, probably due to the framework damage.
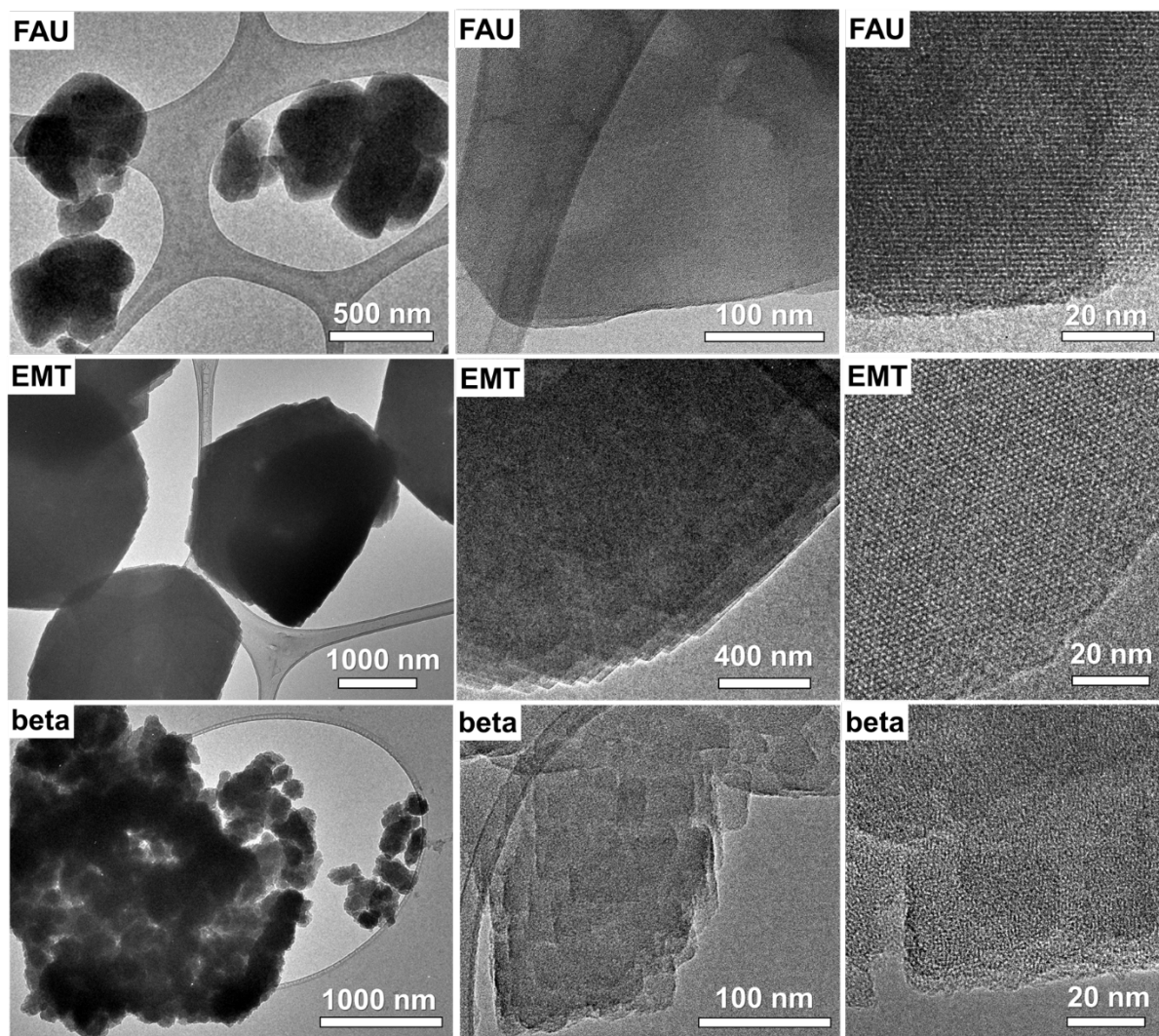
Figure S2. TEM images of carbon samples with various magnifications. Scale bars and lanthanum zeolite templates are shown in each image. All images show no dense deposition of external carbon. For the carbon synthesis, zeolite was heated to 600 °C under dry N_2 flow, using a vertically placed, fused quartz reactor equipped with a fritted disk. A mixture of ethylene gas, N_2 and steam was passed through the zeolite bed at 600 °C. The gas flow was switched to dry N_2 when the carbon deposition was completed. Then, the temperature was increased to 850 °C, and maintained there for 2 h. The resultant product was slurried in a HF/HCl solution, or alternatively conc. hydrochloric acid followed by with hot NaOH solution, to release carbon from template.
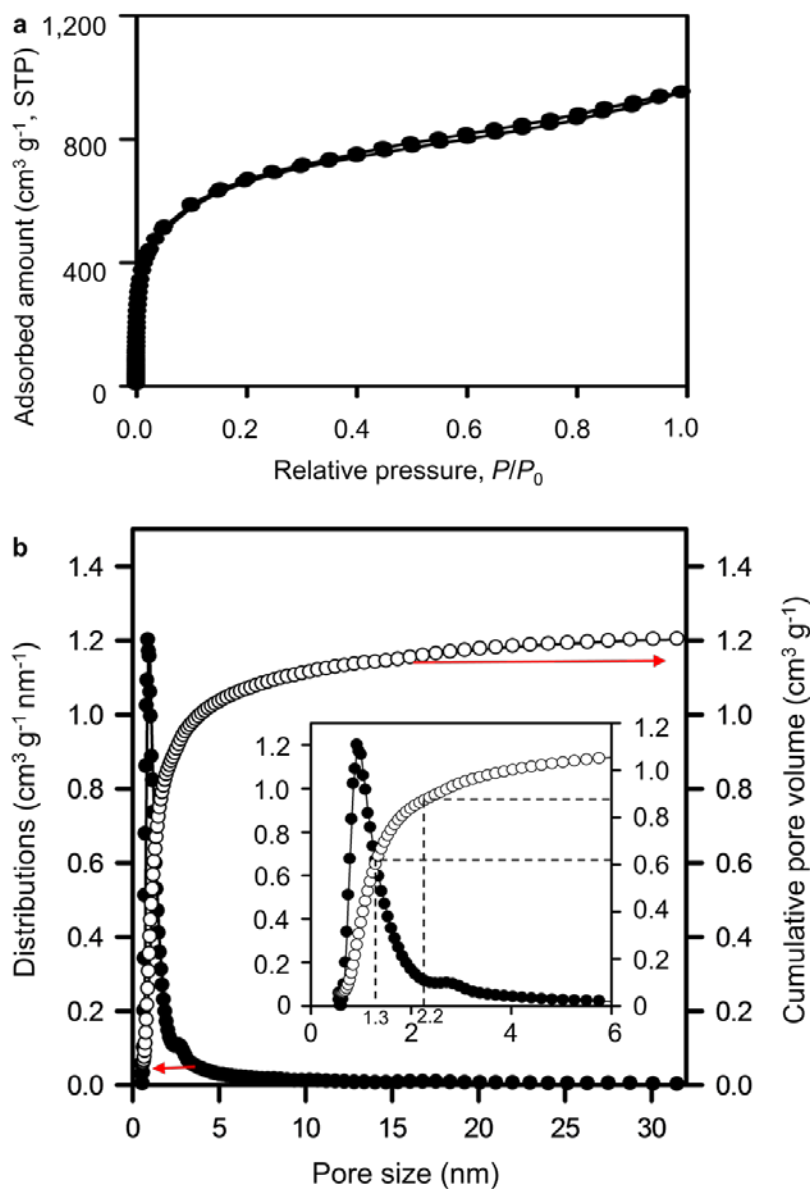
Figure S3. Pore structure analysis of LaY-templated carbon using Ar adsorption. a, Ar adsorption-desorption isotherm at 87 K. **b**, Cumulative pore volume and pore size distributions, calculated using non-linear density functional theory method with a fitting error of 0.7 % (inset : magnified version of the graph in the range of pore diameter from 0 to 6 nm). The pore size distribution can be classified into three categories: diameters less than 1.3 nm as faithfully templated pores, 1.3~2.2 nm as partially templated pores, and greater than 2.2 nm as defective pores. Pore volumes corresponding to the three categories are 0.61, 0.28 and 0.31 cm^3 g^{-1}, respectively. The ratios of their distribution are 7.4: 1.8: 0.8.
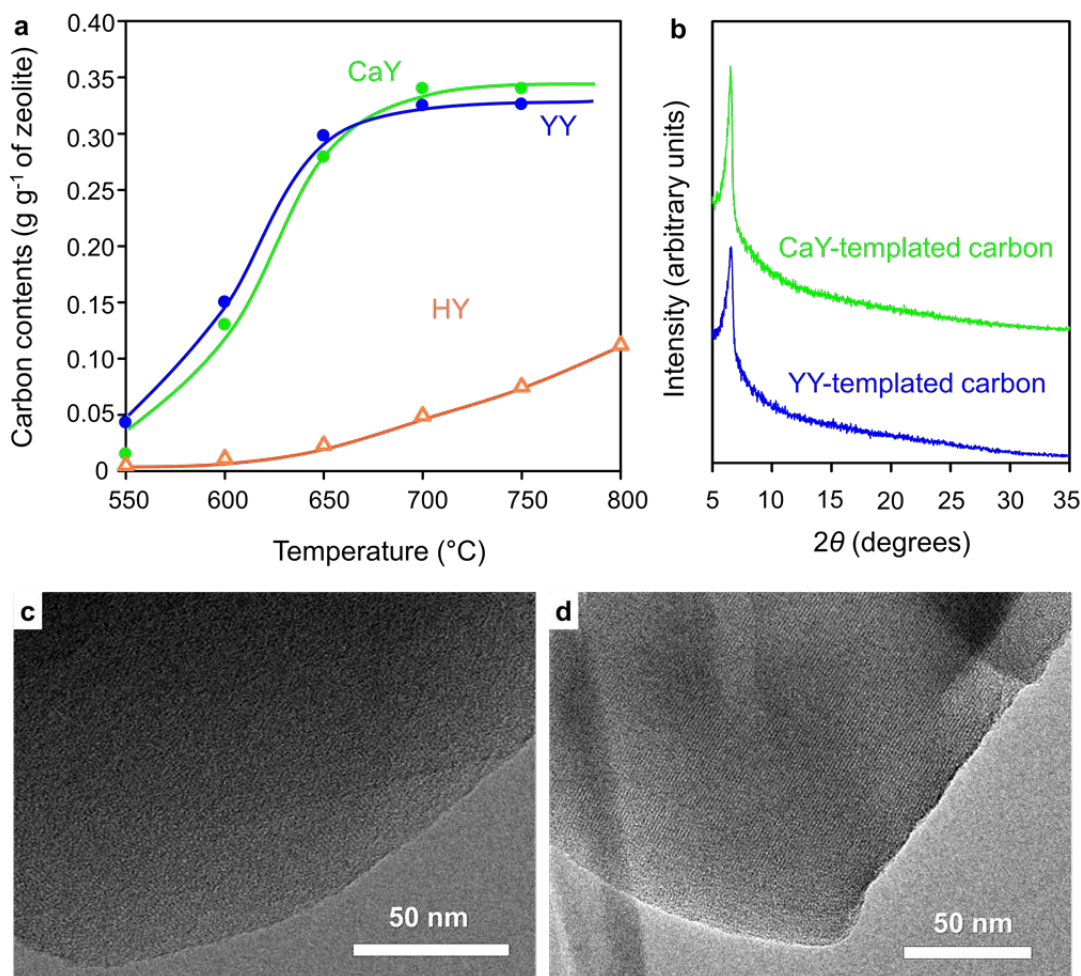
Figure S4. Carbon synthesis using Y^{3+} and Ca^{2+} ion-exchanged zeolite FAU. a, Carbon deposition was performed under the same condition as given in Extended Data Figure 1. This result indicates that Y^{3+} and Ca^{2+} can also lower the carbonization temperature like La^{3+}. **b,** XRD patterns of the resultant carbons liberated from templates according to the procedure given in Figure S2. The XRD patterns exhibit an intense diffraction peak at 6.4°. **c-d,** TEM images of the carbon products synthesized using YY zeolite (**c**) and CaY zeolite (**d**), showing highly ordered microporous structure without external carbon deposition.
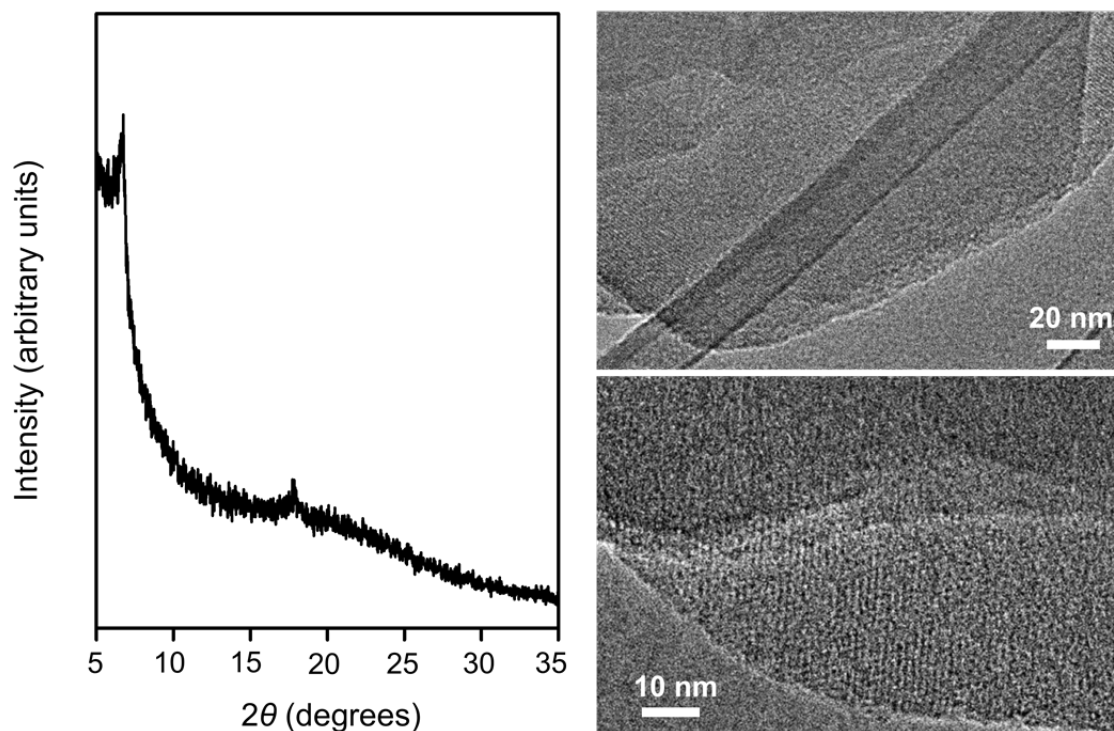
Figure S5. XRD pattern and TEM images of a carbon product, synthesized using acetylene instead of ethylene. The LaY zeolite was heated to 850 °C after carbon deposition only at 340 °C. The carbon product liberated from the LaY zeolite shows the resolved diffraction peak at $2\theta = 6.5°$ in the XRD patterns and lattice fringes in the TEM images. These indicates micropore orders in the carbon.

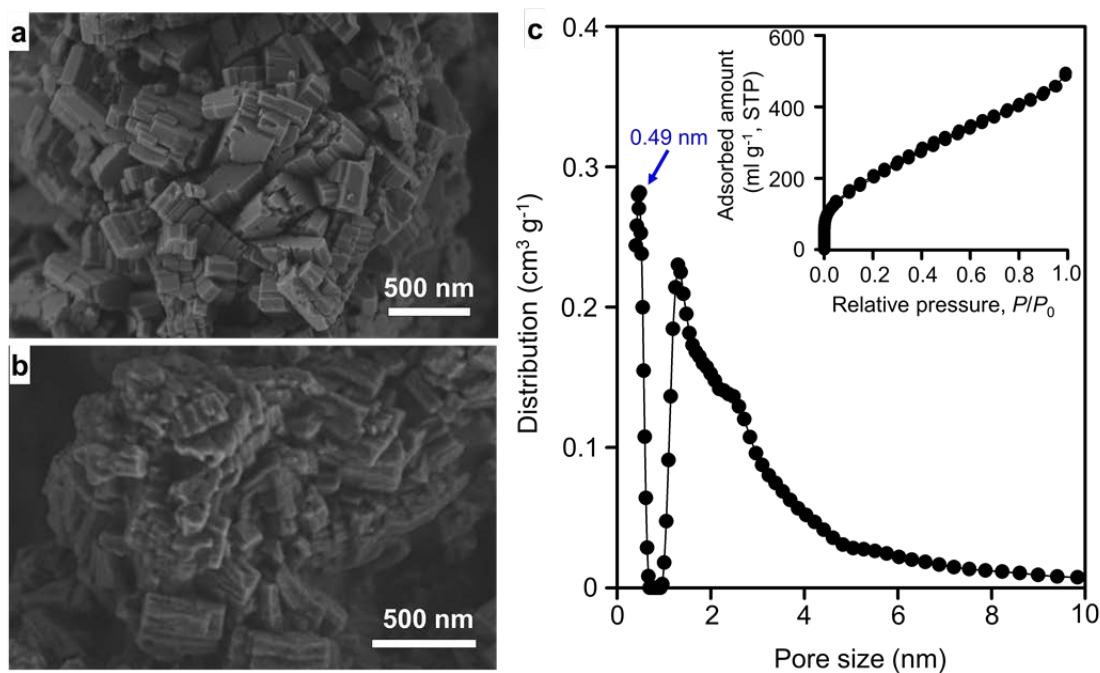**Figure S6. Carbon synthesis results using Ca²⁺ ion-exchanged MFI zeolite as templates.
a** and **b,** SEM images showing similarity in morphologies between zeolite MFI (**a**) and its carbon product (**b**). **c,** pore size distribution of the carbon, calculated from argon adsorption isotherm at -186 °C (inset) by non-local density functional theory. The pores at 0.49 nm correspond to the thickness of the zeolite framework between the nearest neighboring pores, indicating that the narrow zeolite pores were faithfully replicated to carbon frameworks in some regions. Pores larger than 1 nm indicate insufficient formation of carbon frameworks in other regions.
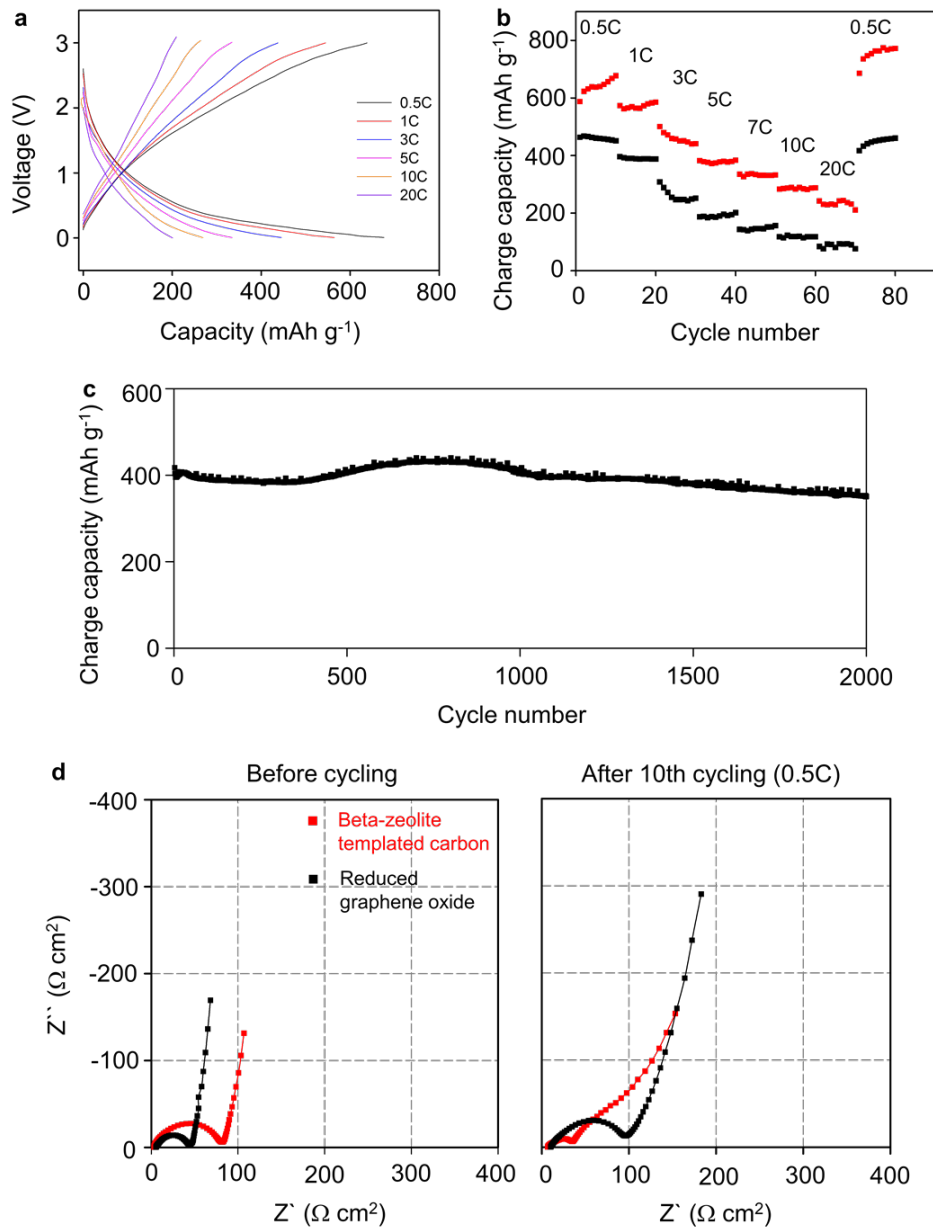
Figure S7. Electrochemical properties of the carbon in lithium battery application. a, Charge-discharge voltage curves of beta-templated carbon at different power rates (1C = 0.4 mA cm^2), indicating that the carbon electrode is operated through mainly adsorption of lithium ions. **b,** Comparison of rate capability between the beta-templated carbon (red) and reduced graphene oxide (rGO) purchased from Ditto tech. (black). The results indicate that the beta-templated carbon exhibits higher capacity and better rate capability than the rGO. **c,** cycle performance of the carbon at a rate of 4C, showing excellent cycle performance with a high capacity. This capacitance stability can be attributed to their rigid 3D porous structure. **d,** Nyquist plot for the beta-zeolite templated carbon and the rGO before and after a galvanostatic charge-discharge cycle. Before the cycle, the charge-transfer resistance of the beta-templated carbon, determined by the diameter of the Z` vs. Z`` semi-circle, is larger than that of the rGO. This may be attributed to chemisorbed oxygen that can be removed during the cycles, or to the presence of 5- or 7-membered rings in the carbon framework that may

lead to a decrease in electronic conductivity. However, the charge-transfer resistance of both electrodes is reversed by cycling the electrodes. This indicates that the resistance of interface between electrolyte and beta-templated carbon electrodes is lower than that formed on the graphene electrode. The result seems to be attributed to low resistance of solid electrolyte interface layer formed on the curved surface of beta-templated carbon. The measurement were performed in a coin type half-cell using pure Li as a counter electrode. The carbon electrodes were prepared by spreading 85 wt% carbon samples, 5 wt% carbon black (super P, TIMCAL Graphite & Carbon) and 10 wt% polyvinylidene fluoride binder (aldrich) onto a Cu current collector and dried in a vaccum oven at 120 °C overnight. The typical loading amount of the carbon samples was ~0.6 mg cm^{-2}. 1 M $LiPF_6$ in a mixture of ethylene carbonate and diethyl carbonate (1:1 in weight) was used as an electrolyte.
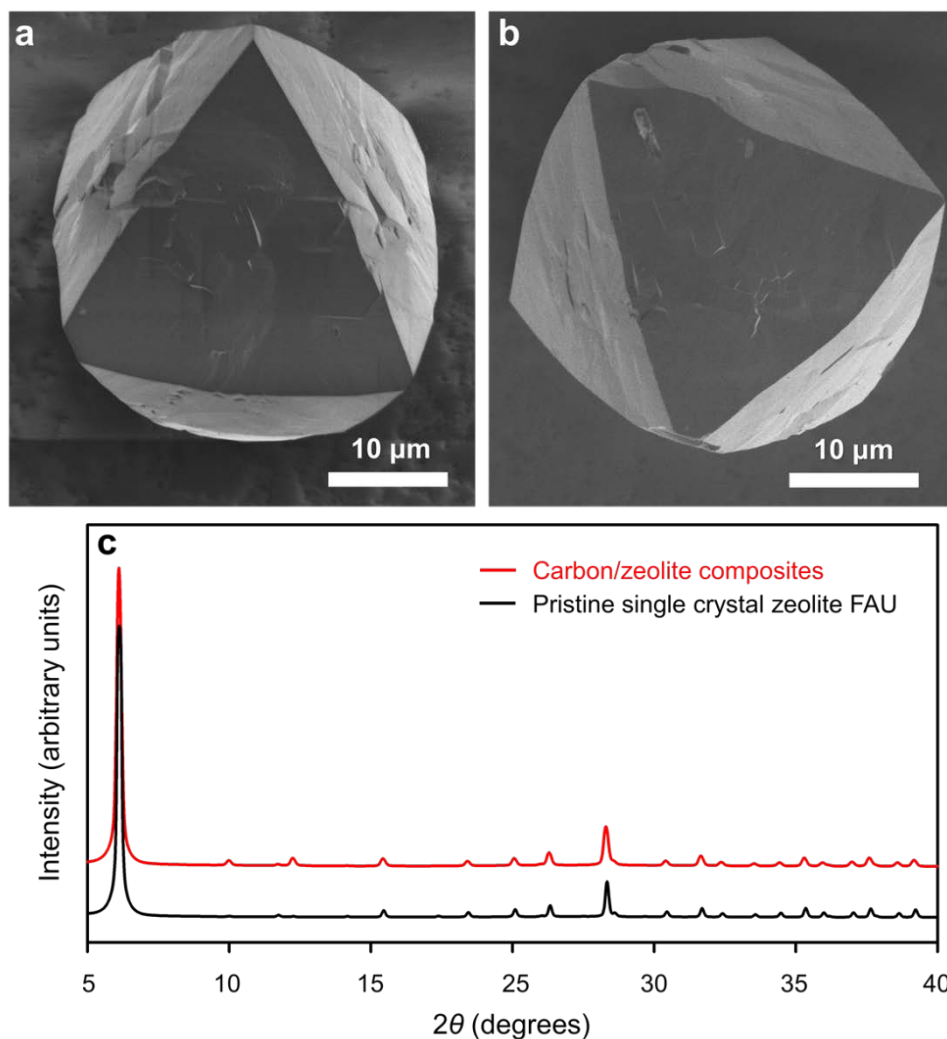
Figure S8. Evidence for no structural damage by carbon deposition into FAU zeolite. a and **b,** SEM images before (**a**) and after (**b**) carbon deposition for 3 h at 600 °C. **c,** Powder XRD patterns before and after the carbon deposition treatment. The patterns was collected with synchrotron radiation in transmission mode using a narrow capillary tube.
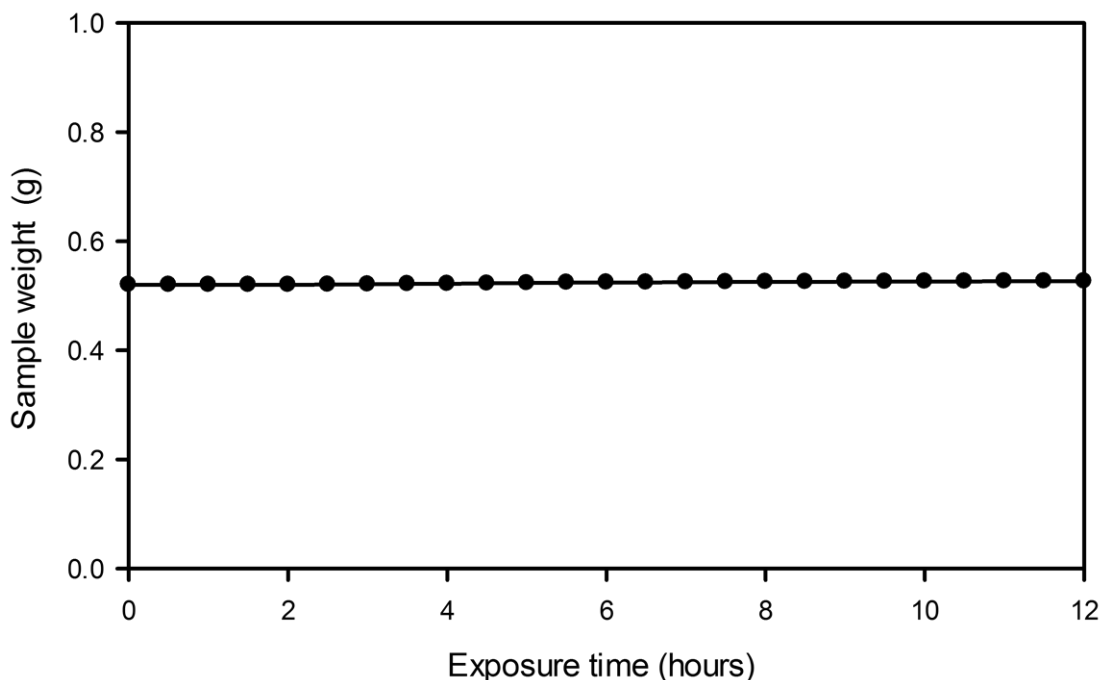
Figure S9. Resistance of Paratone oil-coated carbon-zeolite composite to moisture absorption. Note that zeolite becomes hydrophobic when carbon is deposited in the pores. Furthermore, in the present case, the zeolite pores were so well plugged with carbon that the specific surface area (BET area) decreased to only 7 m^2g^{-1}, which amounted to only 2% of the surface area of a pristine zeolite sample. In such an almost nonporous sample, the moisture uptake was expected to occur very slowly. Besides, for maximum precaution, the sample was coated with hydrophobic Paratone oil. To prove the moisture resistance of the oil-coated sample, the sample weight was monitored during the exposure to a 65% humid N_2 atmosphere, using a high-precision magnetic suspension balance (IsoSORP, Rubotherm). As shown in the present figure, the sample weight changed very little. If the weight change is counted as moisture uptake, the moisture uptake for 12 h under N_2 with 65% relative humidity would become 0.6 x 10^{-2} g H_2O/g zeolite. This is equivalent to only 1.9 x 10^{-2} O atoms per deposited C atom. Note also that XRD measurement was performed under dry N_2 atmosphere to prevent moisture uptakes. Considering all these precautions and the above measured value, it can be ensured that the XRD measurement was performed without moisture problems.